Evaluation of Dual-Energy CT for Differentiating Intracerebral Hemorrhage from Iodinated Contrast Material Staining[1]

Rajiv Gupta, MD, PhD
Catherine M. Phan, MD
Christianne Leidecker, PhD
Thomas J. Brady, MD
Joshua A. Hirsch, MD
Raul G. Nogueira, MD
Albert J. Yoo, MD

Purpose: To evaluate the efficacy of dual-energy computed tomography (CT) in the differentiation of intracerebral hemorrhage (ICH) from iodinated contrast material in patients who received contrast material via intraarterial or intravenous delivery.

Materials and Methods: This retrospective study was approved by the local institutional review board, which waived the informed consent requirement for the analysis. Sixteen patients with acute stroke and two with head trauma who had undergone intraarterial or intravenous administration of iodinated contrast material were evaluated by using dual-energy CT to differentiate areas of hyperattenuation secondary to contrast material staining from those representing ICH. A dual-energy CT scanner was used for imaging at 80 and 140 kV, and a three-material decomposition algorithm was used to obtain virtual unenhanced images and iodine overlay images. The sensitivity, specificity, and accuracy of dual-energy CT in the prospective differentiation of intraparenchymal contrast material from hemorrhage were obtained. Follow-up images were used as the standard of reference.

Results: There were 28 intraparenchymal areas of hyperattenuation classified at dual-energy CT as iodinated contrast material staining ($n = 20$, 71%), hemorrhage ($n = 5$, 18%), or both ($n = 3$, 11%). Two of the three areas of hyperattenuation seen on both virtual unenhanced and iodine overlay images were related to mineralization. The sensitivity, specificity, and accuracy of dual-energy CT in the identification of hemorrhage were 100% (six of six areas), 91% (20 of 22 areas), and 93% (26 of 28 areas), respectively.

Conclusion: Dual-energy CT can help differentiate ICH from iodinated contrast material staining with high sensitivity and specificity in patients who have recently received intraarterial or intravenous iodinated contrast material.

[1] From the Department of Radiology, Massachusetts General Hospital, 55 Fruit St, Neuroradiology GRB-273A, Boston, MA 02114 (R.G., C.M.P., T.J.B., J.A.H., R.G.N., A.J.Y.); and Siemens Medical Solutions, Malvern, Pa (C.L.). Received September 30, 2009; revision requested November 4; revision received December 11; accepted February 3, 2010; final version accepted April 27. **Address correspondence to** C.M.P. (e-mail: *cmphan@partners.org*).

To date, reperfusion therapy is the only proved treatment for acute ischemic stroke (1–3). However, the benefit of this treatment must be balanced against its risks, particularly posttreatment intracerebral hemorrhage (ICH). In general, ICH is more common with intraarterial therapy than with intravenous thrombolysis (1,2,4,5) and can result in significant morbidity and mortality (2,6). Data suggest that clinically significant ICH tends to occur within the first 12–24 hours after treatment (7). Furthermore, it has been demonstrated that there can be an ongoing evolution of hemorrhagic transformation early after treatment, with some patients demonstrating marked worsening (8,9). Therefore, the ability to reliably identify hemorrhagic transformation immediately after therapy would allow for appropriate management (eg, discontinuation or reversal of antithrombotic medication) that may prevent hemorrhage growth (10,11).

Unenhanced head computed tomography (CT) is commonly performed within the first 24 hours after intraarterial therapy to assess for early complications of therapy (12) and has been demonstrated to provide important prognostic information (13,14). Therefore, a common clinical problem is the differentiation of contrast material–related areas of hyperattenuation from acute ICH, as this may influence the decision to continue or initiate antiplatelet or anticoagulation therapy (10).

The purpose of this study was to evaluate the ability of dual-energy CT to enable the differentiation of ICH from iodinated contrast material in patients who underwent contrast material administration by means of intraarterial or intravenous delivery.

Advance in Knowledge

- Dual-energy CT can help accurately differentiate between intraparenchymal hemorrhage and iodinated contrast material staining.

Materials and Methods

Patient Selection

One author (C.L.) is an employee of Siemens Medical Solutions. None of the other authors have a direct or indirect financial interest in the product under investigation. This retrospective study was approved by the institutional review board, which waived the informed consent requirement for the analysis. At our institution, all patients who undergo conventional angiography for intraarterial embolectomy or thrombolysis are evaluated with unenhanced CT immediately after the procedure to assess for any treatment-related complications. Because the dual-energy CT scanner was not available for use in all patients, a subset of these patients (18 of 55; 33%) underwent imaging with the dual-energy protocol. The patients were prospectively screened and retrospectively analyzed on the basis of the availability of follow-up images to establish the status of each observed area of high attenuation.

Between October 2008 and March 2010, 18 patients (mean age, 67 years; range, 36–93 years) were referred for dual-energy CT. There were 10 men (mean age, 64 years; range, 36–93 years) and eight women (mean age, 70 years; range, 50–84 years). There was no significant difference in age between men and women (P = .55). Three patients were excluded from analysis because of the lack of follow-up images. In 13 of the 15 remaining patients, imaging was performed within 30 minutes of the end of the interventional procedure (conventional angiography for intraarterial reperfusion therapy [n = 12] or carotid stent placement [n = 1]). Two of the 15 patients underwent a dual-energy evaluation to further assess a new intraparenchymal area of hyperattenuation that was observed on a routine unenhanced CT scan. Dual-energy CT was performed to determine if this area of hyperattenuation represented hemorrhage or contrast material staining from a previous CT angiographic examination. Four of the 15 patients were excluded because the observed intracranial area of hyperattenuation was not intraparenchymal. In summary, only 11 of the 18 patients who underwent dual-energy CT demonstrated intracerebral hyperattenuation with adequate follow-up imaging.

Implications for Patient Care

- Preliminary evidence suggests that dual-energy CT can help reliably differentiate intraparenchymal hemorrhage from iodinated contrast material in patients who have recently received intraarterial or intravenous iodinated contrast material.
- This differentiation is particularly important immediately after intraarterial stroke therapy, especially when anticoagulation or antiplatelet therapy is being considered.

Dual-Energy CT

All patients were scanned with a dual-source CT unit (Somatom Definition; Siemens Healthcare, Forchheim, Germany) operated in the dual-energy mode, with tube A at 80 kV and 499 mA, tube B at 140 kV and 118 mA (effective milliampere seconds of 714 and 168, respectively), and a collimation of 14 × 1.2 mm. The total effective dose of approximately 3 mSv was similar to that of conventional head CT.

Published online before print
10.1148/radiol.10091806

Radiology 2010; 257:205–211

Abbreviation:
ICH = intracerebral hemorrhage

Author contributions:
Guarantors of integrity of entire study, R.G., C.M.P., T.J.B., A.J.Y.; study concepts/study design or data acquisition or data analysis/interpretation, all authors; manuscript drafting or manuscript revision for important intellectual content, all authors; manuscript final version approval, all authors; literature research, R.G., C.M.P., C.L., A.J.Y.; clinical studies, R.G., C.M.P., C.L., R.G.N., A.J.Y.; statistical analysis, R.G., C.M.P., A.J.Y.; and manuscript editing, R.G., C.M.P., C.L., J.A.H., R.G.N., A.J.Y.

See Materials and Methods for pertinent disclosures.

Figure 1

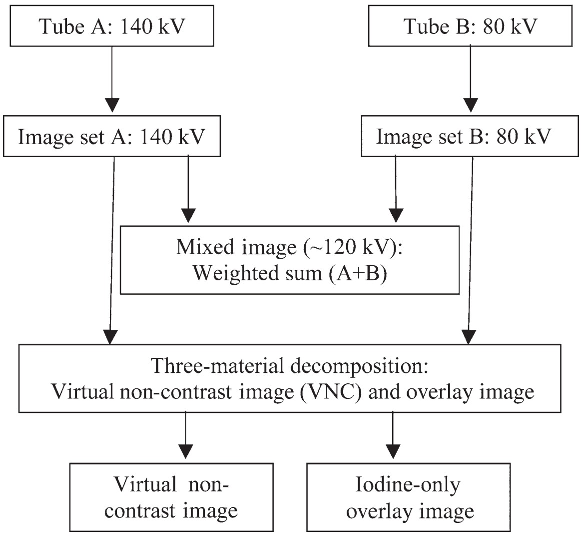

Figure 1: Flow diagram for dual-energy CT processing. Any three preselected materials (eg, brain parenchyma, hemorrhage, and iodine) can be differentiated at a pixel-by-pixel level.

Table 1

Different Patterns of Hyperattenuation on Virtual Unenhanced and Iodine Overlay Images

Diagnosis	Virtual Unenhanced Images	Iodine Overlay Images
Hemorrhage	+	−
Iodinated contrast material staining	−	+
Both hemorrhage and contrast material staining	+	+
Calcium, mineralization	+	+

Note.—Images were obtained with dual-energy software (Syngo Dual Energy Brain Hemorrhage). + = Hyperattenuation present, − = hyperattenuation absent.

Figure 2

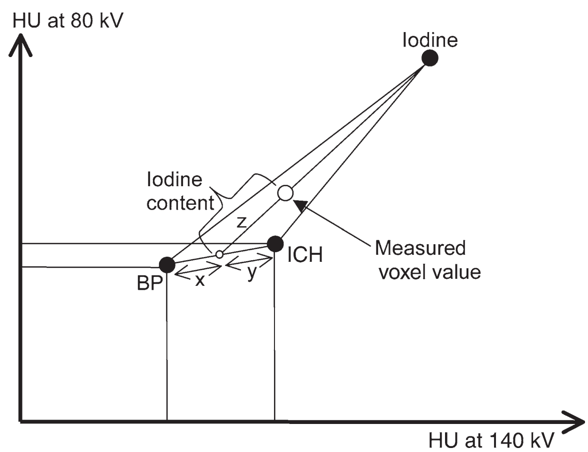

Figure 2: Principle of the three-material decomposition of a voxel used by the dual-energy software. This software splits every voxel in the 80- and 140-kV image pair into three components represented by brain parenchyma (*BP*), hemorrhage (*ICH*), and iodine, which are empirically estimated: The intercepts x and y correspond to the portion of brain parenchyma and ICH in the voxel, whereas the intercept z along the iodine axis represents the iodine content of the voxel on this two-energy plot. To the extent the measured value of a voxel does not conform to a mixture of brain parenchyma and ICH, the difference can be attributed to iodine. The virtual unenhanced images display the noniodine component of the voxel (ie, the brain parenchyma and ICH represented by x and y), and the overlay images display the z intercept (ie, the iodine content).

Two image sets with 4.0- and 1.5-mm-thick sections were reconstructed by using H30 (medium smooth) and D37s (dual-energy, medium sharp) kernels, respectively. Each image set consisted of an 80-kV series, a 140-kV series, and a so-called "single-energy" series, which combined the 80- and 140-kV images to simulate an image obtained at 120 kV. The single-energy series has a higher signal-to-noise ratio than the constituent 80- and 140-kV image sets (Fig 1).

Dual-energy postprocessing was performed on the 1.5-mm-thick data set by using dedicated software (Syngo Dual Energy Brain Hemorrhage; Siemens Healthcare) (15,16) that employs a three-material decomposition algorithm based on brain parenchyma, hemorrhage, and iodine as the three preselected materials. This process is schematically shown in Figure 2. A virtual unenhanced image and an iodine overlay image were derived from the original 80- and 140-kV data sets.

Image Analysis

Image analysis was performed in consensus by three experienced radiologists with 8 (R.G., C.M.P.) and 9 (A.J.Y.) years of experience. Among the intracerebral areas of hyperattenuation seen on the simulated 120-kV images, only intraparenchymal areas of hyperattenuation were prospectively analyzed and classified as hemorrhage, contrast material, or a combination of both on the basis of the virtual unenhanced and iodine overlay images (Table 1). Imaging analysis for each case was completed before the follow-up images became available.

Follow-up images from either unenhanced CT or magnetic resonance (MR) imaging were used to determine the ground truth about each area of hyperattenuation observed on the dual-energy CT scan. The finding of washout or near-complete clearing of the area of hyperattenuation in 24–48 hours at unenhanced CT was used as evidence that the area of hyperattenuation represented contrast material staining (9,14,17,18). If the area of hyperattenuation persisted for more than 48 hours and developed a characteristic rim of hypoattenuation (presumed to be edema or infarct), it was classified as hemorrhage. The 48-hour cutoff is what we routinely use in our clinical practice. When susceptibility-weighted

Table 2

Criteria used for True-Positive, False-Positive, True-Negative, and False-Negative Findings of Hemorrhage at Dual-Energy CT and Follow-up Imaging

	Findings at Dual-Energy CT*		Findings at Follow-up†	
Diagnosis	Virtual Unenhanced Images	Iodine Overlay Images	CT	MR Imaging
True positive (*n* = 6)	+	±	Persistent hyperattenuation	Susceptibility artifact
False positive (*n* = 2)	+	±	Near-complete washout	No susceptibility artifact in the area of hyperattenuation
True negative (*n* = 20)	−	+	Near-complete washout	No susceptibility artifact in the area of hyperattenuation
False negative (*n* = 0)	−	+	Persistent hyperattenuation	Susceptibility artifact

* + = Positive for hyperattenuation, − = negative for hyperattenuation, ± = positive or negative for hyperattenuation.

† Follow-up imaging was performed 24–48 hours after treatment.

Figure 3

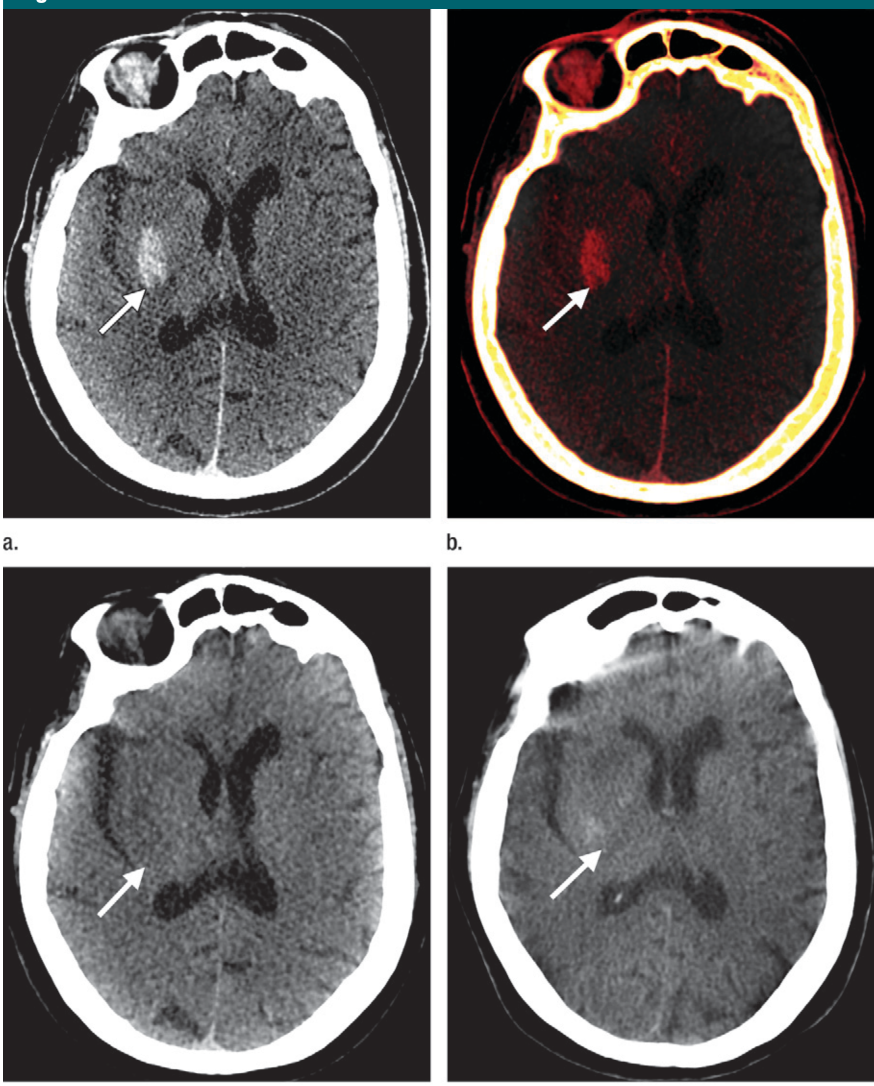

a. b. c. d.

Figure 3: Intraparenchymal areas of hyperattenuation due to iodinated contrast material staining of infarcted brain parenchyma in a 78-year-old woman who underwent successful recanalization of the intracranial bifurcation of the right internal carotid artery. **(a)** Single-energy CT scan shows an intraparenchymal area of hyperattenuation (arrow) in the right lentiform nucleus. **(b)** Iodine overlay image shows that this area of hyperattenuation corresponds to an area of diffuse contrast material staining (arrow). **(c)** Virtual unenhanced image shows an area of subtle hypoattenuation (arrow) related to the infarct. **(d)** Follow-up unenhanced CT scan demonstrates near-complete washout of the contrast material (arrow).

MR images were available, they were used as the reference standard.

Statistical Analysis

We analyzed the presence or absence of intraparenchymal hemorrhage on the dual-energy CT scans and the follow-up images (the standard of reference). Areas classified as hemorrhage alone or as a combination of hemorrhage and iodine at dual-energy CT were considered positive for hemorrhage. True-positive, false-positive, true-negative, and false-negative findings were derived for the detection of ICH with dual-energy CT according to the criteria given in Table 2. Sensitivity, specificity, and accuracy were computed by using software (MedCalc, version 10.0; MedCalc, Mariakerke, Belgium).

Figure 4

a.

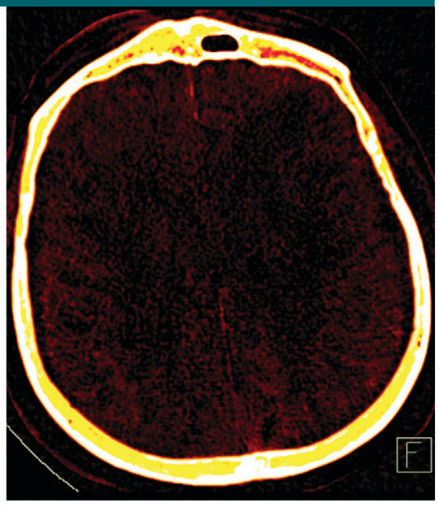

b.

c.

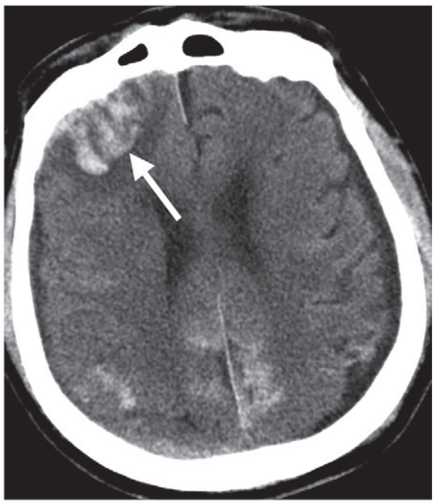

d.

Figure 4: Right frontal intraparenchymal hyperattenuation due to hemorrhage in a 64-year-old man referred for acute head trauma; intravenous contrast material had been previously administered. **(a)** Single-energy CT scan shows right frontal intraparenchymal hyperattenuation (arrow) and other scattered areas of bilateral subarachnoid hyperattenuation. **(b)** Iodine overlay image shows that there is no corresponding area of hyperattenuation. **(c)** Virtual unenhanced image clearly shows the foci of hyperattenuation (arrow), which are suggestive of intracranial hemorrhage. **(d)** Unenhanced CT scan obtained at 48-hour follow-up demonstrates stable hyperattenuation in the right frontal lobe, with an increase in the surrounding edema. This finding helps confirm the original dual-energy CT diagnosis of intraparenchymal hemorrhage.

Results

Twenty-eight areas of intraparenchymal hyperattenuation were identified on the single-energy scans. Dual-energy CT scans were evaluated according to the criteria given in Table 1, and the areas of hyperattenuation were prospectively classified as iodinated contrast material staining alone (*n* = 20, 71%; Fig 3), hemorrhage alone (*n* = 5, 18%; Fig 4), or a combination of contrast material and hemorrhage (*n* = 3, 11%).

All 20 areas of hyperattenuation classified as contrast material alone at dual-energy CT were demonstrated to have no hemorrhage at follow-up imaging (Table 3), as determined by means of complete washout, lack of susceptibility artifacts, or both. All five areas of hyperattenuation classified as hemorrhage alone with dual-energy CT were confirmed as such on subsequent images. Of the three areas classified as a combination of contrast material and hemorrhage, one was demonstrated to have a hemorrhagic component. The other two cases were found to be areas of mineralization, as determined with available previous images (Table 3). Except for those areas of mineralization, all other areas of hyperattenuation (26 of 28) were correctly classified prospectively with dual-energy CT for the presence versus absence of hemorrhage, for an accuracy of 93%. The sensitivity and specificity for the presence of hemorrhage were 100% (six of six areas; 95% confidence interval: 54.1%, 100%) and 91% (20 of 22 areas; 95% confidence interval: 70.8%, 98.6%), respectively.

Discussion

Hemorrhagic transformation is a major complication of reperfusion therapy for acute ischemic stroke. Rates of symptomatic ICH obtained in the major trials of intraarterial therapy (2,4,8) range from 6.3% to 10.9%. Parenchymal hematomas, defined as ICH with associated mass effect, have been shown to have a negative effect on both short- and long-term clinical outcomes (6,19). Currently, unenhanced CT is the standard of care for the detection of ICH (20) and is performed soon after intraarterial therapy to assess for procedural complications. Parenchymal contrast enhancement or contrast material extravasation is a common finding after intraarterial therapy, occurring in 30%–50% of cases (9,14,17,21). ICH and contrast material staining may appear identical on unenhanced CT scans. If the attenuation value of an area of hyperattenuation exceeds that expected for hemorrhage, it can be confidently assumed that there is a component of iodinated contrast material within it. In this study, only a minority of the intraparenchymal areas of hyperattenuation (*n* = 4, 16%) demonstrated such

Table 3

Comparison of Findings at Dual-Energy CT and Follow-up Imaging

	Appearance at Dual-Energy CT*			Interpretation	
Diagnosis	Single-Energy Images†	Virtual Unenhanced Images	Iodine Overlay Images	Dual-Energy CT	Follow-up Unenhanced CT/MR Imaging
Hemorrhage only ($n = 5$)	+	+	−	Hemorrhage alone	Hemorrhage (CT: $n = 2$; MR imaging: $n = 3$)
Iodinated contrast material staining only ($n = 20$)	+	−	+	Contrast material alone	No hemorrhage (CT: $n = 5$; MR imaging: $n = 15$)
Mixed hemorrhage and contrast material or mineralization ($n = 3$)	+	+	+	Both hemorrhage and contrast material	Hemorrhage (CT: $n = 1$), mineralization ($n = 2$)‡

* + = Hyperattenuation present, − = hyperattenuation absent.

† For single-energy images, the 80- and 140-kV images were combined to simulate an image equivalent to one obtained at 120 kV.

‡ Mineralization was found in two cases on the basis of previously obtained images.

markedly elevated attenuation levels (eg, ≥120 HU). Even in these cases, one cannot assume that there is not associated hemorrhage; for example, dual-energy CT depicted superimposed hemorrhage in one of the four cases (25%). Definitive identification of extravascular contrast material requires serial imaging to demonstrate early washout (within 24–48 hours) in the hyperattenuating lesion (9,14,17,18). Hemorrhage is persistent over several days to weeks. This study provides a method for prospectively determining the status of each area of hyperattenuation on an unenhanced CT scan.

The tissue characterization capabilities of dual-energy CT have been previously studied (22–30). In this initial study, we have demonstrated that dual-energy CT can help accurately differentiate intraparenchymal hemorrhage from iodinated contrast material staining. The discriminatory power of dual-energy CT comes at no extra cost in terms of radiation dose or image quality as compared with single-energy unenhanced CT. Our results confirm the findings of a recent study (26), which demonstrated that iodine could be effectively subtracted from a dual-energy CT angiogram to yield a virtual unenhanced image that rivaled traditional unenhanced CT in its diagnostic utility for hemorrhage detection.

Given the limited distribution of dual-energy CT scanners at the present time and the increasing use of intraarterial therapy resulting in contrast material staining and/or extravasation, the dilemma of how to treat these patients clinically is quite real. Susceptibility-weighted MR imaging remains an option for identifying the presence or absence of hemorrhage after intraarterial therapy (10) even though it is somewhat limited by availability, the presence of pacemakers and other MR imaging–incompatible devices, and the overall difficulty of transporting an acutely sick patient to the MR imaging suite. Another option is to “simulate” a dual-energy scanner by using a single-source, single-energy scanner. If, in an axial step-and-shoot mode, 80- and 140-kV sections are obtained at each table position, one can postprocess the data set by using the dual-energy CT techniques described herein. Because these 80- and 140-kV images will be displaced in time by the time it takes for one gantry rotation, patient motion may introduce misregistration artifacts. However, on a modern gantry with a rotation time of approximately 0.27–0.33 second, this time difference may not pose a severe problem. Further scanner and appropriate postprocessing software development are necessary to clinically realize this option.

When interpreting these results, it is important to be aware of certain limitations. Dual-energy CT can only help differentiate up to three preselected materials because of fundamental physics of how attenuation is affected by the Compton and photoelectric effects. If a hyperattenuating pixel consists of four or more materials, without any a priori knowledge, dual-energy CT cannot help differentiate the constituent materials. For example, a focus of calcification (eg, skull and other areas of parafalcine and choroid plexus calcification) will appear as an area of hyperattenuation on both the virtual unenhanced and iodine overlay images; such a case cannot be differentiated from a combination of hemorrhage and contrast material on the basis of the results of dual-energy CT analysis. Previously obtained images are needed to make this discrimination. Certain artifacts at CT (eg, beam hardening or metallic artifacts) may also confound dual-energy analysis. For objects with a very high attenuation (eg, undiluted contrast material) that do not change substantially between 80- and 140-kV images, dual-energy analysis may fail.

All of the above situations could lead to false-negative or false-positive conclusions regarding the presence of hemorrhage. In the small cohort of patients studied herein, these potential limitations did not pose a substantial problem: Dual-energy CT enabled correct classification in 26 of 28 instances of intraparenchymal hyperattenuation, with calcification as the main confounder. Although this finding is reassuring, it may not be applicable to all possible scenarios; a larger trial is needed to determine the sensitivity, specificity, and false-positive and/or false-negative rates of dual-energy CT in the assessment of ICH after intraarterial therapy.

In conclusion, dual-energy CT has high sensitivity and specificity in the differentiation of intracranial hemorrhage from iodinated contrast material staining and may be particularly helpful in patients who have recently undergone intraarterial stroke therapy.

References

1. Tissue plasminogen activator for acute ischemic stroke. The National Institute of Neurological Disorders and Stroke rt-PA Stroke Study Group. N Engl J Med 1995;333(24):1581–1587.
2. Furlan A, Higashida R, Wechsler L, et al. Intra-arterial prourokinase for acute ischemic stroke: the PROACT II study—a randomized controlled trial. Prolyse in Acute Cerebral Thromboembolism. JAMA 1999;282(21):2003–2011.
3. Rha JH, Saver JL. The impact of recanalization on ischemic stroke outcome: a meta-analysis. Stroke 2007;38(3):967–973.
4. Smith WS, Sung G, Saver J, et al. Mechanical thrombectomy for acute ischemic stroke: final results of the Multi MERCI trial. Stroke 2008;39(4):1205–1212.
5. Lees KR, Zivin JA, Ashwood T, et al. NXY-059 for acute ischemic stroke. N Engl J Med 2006;354(6):588–600.
6. Berger C, Fiorelli M, Steiner T, et al. Hemorrhagic transformation of ischemic brain tissue: asymptomatic or symptomatic? Stroke 2001;32(6):1330–1335.
7. Khatri P, Wechsler LR, Broderick JP. Intracranial hemorrhage associated with revascularization therapies. Stroke 2007;38(2):431–440.
8. IMS Study Investigators. Combined intravenous and intra-arterial recanalization for acute ischemic stroke: the Interventional Management of Stroke Study. Stroke 2004;35(4):904–911.
9. Jang YM, Lee DH, Kim HS, et al. The fate of high-density lesions on the non-contrast CT obtained immediately after intra-arterial thrombolysis in ischemic stroke patients. Korean J Radiol 2006;7(4):221–228.
10. Greer DM, Koroshetz WJ, Cullen S, Gonzalez RG, Lev MH. Magnetic resonance imaging improves detection of intracerebral hemorrhage over computed tomography after intra-arterial thrombolysis. Stroke 2004;35(2):491–495.
11. Intracerebral hemorrhage after intravenous t-PA therapy for ischemic stroke. The NINDS t-PA Stroke Study Group. Stroke 1997;28(11):2109–2118.
12. Technology Assessment Committees of the American Society of Interventional and Therapeutic Neuroradiology; Society of Interventional Radiology. Trial design and reporting standards for intraarterial cerebral thrombolysis for acute ischemic stroke. 2003. J Vasc Interv Radiol 2003;14(8):945–946.
13. Leigh R, Zaidat OO, Suri MF, et al. Predictors of hyperacute clinical worsening in ischemic stroke patients receiving thrombolytic therapy. Stroke 2004;35(8):1903–1907.
14. Yoon W, Seo JJ, Kim JK, Cho KH, Park JG, Kang HK. Contrast enhancement and contrast extravasation on computed tomography after intra-arterial thrombolysis in patients with acute ischemic stroke. Stroke 2004;35(4):876–881.
15. Johnson TR, Nikolaou K, Wintersperger BJ, et al. Dual-source CT cardiac imaging: initial experience. Eur Radiol 2006;16(7):1409–1415.
16. Petersilka M, Bruder H, Krauss B, Stierstorfer K, Flohr TG. Technical principles of dual source CT. Eur J Radiol 2008;68(3):362–368.
17. Mericle RA, Lopes DK, Fronckowiak MD, Wakhloo AK, Guterman LR, Hopkins LN. A grading scale to predict outcomes after intra-arterial thrombolysis for stroke complicated by contrast extravasation. Neurosurgery 2000;46(6):1307–1314, discussion 1314–1315.
18. Nakano S, Iseda T, Yoneyama T, Wakisaka S. Early CT signs in patients with acute middle cerebral artery occlusion: incidence of contrast staining and haemorrhagic transformations after intra-arterial reperfusion therapy. Clin Radiol 2006;61(2):156–162.
19. Paciaroni M, Agnelli G, Corea F, et al. Early hemorrhagic transformation of brain infarction: rate, predictive factors, and influence on clinical outcome: results of a prospective multicenter study. Stroke 2008;39(8):2249–2256.
20. Adams HP Jr, del Zoppo G, Alberts MJ, et al. Guidelines for the early management of adults with ischemic stroke: a guideline from the American Heart Association/American Stroke Association Stroke Council, Clinical Cardiology Council, Cardiovascular Radiology and Intervention Council, and the Atherosclerotic Peripheral Vascular Disease and Quality of Care Outcomes in Research Interdisciplinary Working Groups: The American Academy of Neurology affirms the value of this guideline as an educational tool for neurologists. Circulation 2007;115(20):e478–e534.
21. Yokogami K, Nakano S, Ohta H, Goya T, Wakisaka S. Prediction of hemorrhagic complications after thrombolytic therapy for middle cerebral artery occlusion: value of pre- and post-therapeutic computed tomographic findings and angiographic occlusive site. Neurosurgery 1996;39(6):1102–1107.
22. Graser A, Johnson TR, Chandarana H, Macari M. Dual energy CT: preliminary observations and potential clinical applications in the abdomen. Eur Radiol 2009;19(1):13–23.
23. Graser A, Johnson TR, Hecht EM, et al. Dual-energy CT in patients suspected of having renal masses: can virtual nonenhanced images replace true nonenhanced images? Radiology 2009;252(2):433–440.
24. Ruzsics B, Lee H, Zwerner PL, Gebregziabher M, Costello P, Schoepf UJ. Dual-energy CT of the heart for diagnosing coronary artery stenosis and myocardial ischemia-initial experience. Eur Radiol 2008;18(11):2414–2424.
25. Thieme SF, Johnson TR, Lee C, et al. Dual-energy CT for the assessment of contrast material distribution in the pulmonary parenchyma. AJR Am J Roentgenol 2009;193(1):144–149.
26. Ferda J, Novák M, Mírka H, et al. The assessment of intracranial bleeding with virtual unenhanced imaging by means of dual-energy CT angiography. Eur Radiol 2009;19(10):2518–2522.
27. Chandarana H, Godoy MC, Vlahos I, et al. Abdominal aorta: evaluation with dual-source dual-energy multidetector CT after endovascular repair of aneurysms—initial observations. Radiology 2008;249(2):692–700.
28. Stolzmann P, Scheffel H, Rentsch K, et al. Dual-energy computed tomography for the differentiation of uric acid stones: ex vivo performance evaluation. Urol Res 2008;36(3–4):133–138.
29. Lell MM, Hinkmann F, Nkenke E, et al. Dual energy CTA of the supraaortic arteries: technical improvements with a novel dual source CT system. Eur J Radiol doi:10.1016/j.ejrad.2009.09.022. Published online October 8, 2009.
30. Choi HK, Al-Arfaj AM, Eftekhari A, et al. Dual energy computed tomography in tophaceous gout. Ann Rheum Dis 2009;68(10):1609–1612.